Energy Storage Materials 45 (2022) 768–776

Contents lists available at ScienceDirect

Energy Storage Materials

journal homepage: www.elsevier.com/locate/ensm

# Direct conversion of degraded $LiCoO_2$ cathode materials into high-performance $LiCoO_2$: A closed-loop green recycling strategy for spent lithium-ion batteries

Junxiong Wang[a,b], Zheng Liang[a,*], Yun Zhao[b], Jinzhi Sheng[b], Jun Ma[b], Kai Jia[a], Baohua Li[b], Guangmin Zhou[b,*], Hui-Ming Cheng[b,c]

[a] Frontiers Science Center for Transformative Molecules, School of Chemistry and Chemical Engineering, Shanghai Jiao Tong University, Shanghai 200240, China
[b] Shenzhen Geim Graphene Center, Tsinghua Shenzhen International Graduate School, Tsinghua University, Shenzhen 518055, China
[c] Shenzhen Institute of Advanced Technology, Chinese Academy of Science, Shenzhen 518055, China

ARTICLE INFO

*Keywords:*
Energy storage
Lithium-ion batteries
Closed-loop recycling
Lithium cobalt oxides
Spent cathode materials
Regeneration of degraded $LiCoO_2$

ABSTRACT

Lithium cobalt oxide ($LiCoO_2$) is the most widely used cathode materials for smart phones and laptop batteries. With the rapid development of portable electronics, more than 100,000 tons of spent lithium-ion batteries (LIBs) are produced every year. Conventional battery recycling processes including pyrometallurgical and hydrometallurgical processes mainly aim at extracting valuable metallic components from spent LIB cathodes, which requires high temperature reduction and/or acid/alkali chemicals to destroy covalent bond in cathodes and convert them into atoms for further extraction. The former leads to high energy consumption and the latter produces a lot of wastewater, which not only increases cost, but also damages our environment. Moreover, traditional recycling starts from spent battery cathodes and ends up with lithium/cobalt salts, which is unsustainable. Herein, a different recycling strategy to directly convert degraded $LiCoO_2$ into high-voltage $LiCoO_2$ cathode materials was proposed, featuring a closed-loop and green procedure. The directly-converted $LiCoO_2$ from spent cathodes exhibits excellent cyclability at 4.5 V with a high capacity retention of 97.4% after 100 cycles, even superior than pristine $LiCoO_2$. The recovery efficiencies of lithium and cobalt reach 91.3% and 93.5%, respectively, and the energy consumption could be greatly reduced since the roasting temperature was dropped below 400 °C with the assistance of ammonium sulfate. Due to the utilization of low-cost reagents and water as the leaching agent, the potential benefit of the recovery process was estimated to reach 6.94 $/kg cell.

## 1. Introduction

Lithium cobalt oxide ($LiCoO_2$, LCO) with high specific volumetric energy density and stable cyclability dominates lithium-ion battery (LIB) cathodes for portable electronic devices [1–3]. With the development and popularization of these portable devices, a considerable quantity of spent LIBs with LCO cathodes is generated every year. It is worth noting that Li and Co have dual characteristics of both metallic resources and heavy metal pollutants [4–7]. Therefore, the recycling of spent $LiCoO_2$ has raised extensive attention recently [8,9].

The conventional recycling processes for $LiCoO_2$ could be primarily divided into two categories: pyrometallurgical and hydrometallurgical processes [10–12]. Both processes can be summarized as two steps, i.e., structural destruction of cathode into atomic level and extraction of valuable components from it. $LiCoO_2$ is generally prepared through high temperature sintering at approximately 1000 °C, resulting in a robust structure that is quite difficult to be decomposed [13]. Therefore, extreme conditions are required to decompose $LiCoO_2$ into atoms. For example, in pyrometallurgical process, a reduction roasting step at elevated temperatures (approximately 1000 °C) with the addition of reduction reagents is commonly used [14–16]. During this process, lithium and aluminum components become a slag, while cobalt and copper form mixed alloys, which requires further extraction and separation. Alkali and precipitating agents, such as sodium carbonate, are often used in the subsequent extraction and separation step. As for hydrometallurgical process, strong acids are used together with typical reducing agents, generally $H_2O_2$ to create a reducing acidic environment to dissolve $LiCoO_2$ into $Li^+$ and $Co^{2+}$ ions [17]. Almost all types of acids including inorganic acids (sulfuric acid [18], hydrochloric acid [19], nitric acid [20], etc.) and organic acids (methanesulfonic acid [21], citric acid [22], ascorbic acid [23,24], maleic acid [25], oxalic acid [26], etc.) have been applied to dissolve $LiCoO_2$ under certain conditions, where stirring, heating and shaking are involved. During leaching step, a high liquid/solid ratio

* Corresponding authors.
*E-mail addresses:* liangzheng06@sjtu.edu.cn (Z. Liang), guangminzhou@sz.tsinghua.edu.cn (G. Zhou).

https://doi.org/10.1016/j.ensm.2021.12.013
Received 8 September 2021; Received in revised form 29 October 2021; Accepted 11 December 2021
Available online 14 December 2021

(even >10/1) is required to ensure high leaching efficiency, which produces a lot of acidic waste-water [8,9]. The acidic wastewater must be neutralized before disposal, which undoubtedly leads to extra cost and procedures in practical applications. In addition, utilization of alkali is commonly required during the following extraction and separation of $Li^+$ and $Co^{2+}$ after leaching. Obviously, whether from pyro- or hydro-route, elevated temperature and extensive utilization of corrosive agents are greatly unfavorable to a sustainable battery recycling system.

Recently, some salts, such as ammonium chloride and sodium persulfate, have been introduced to the reduction roasting step and proved effective in significantly lowering the decomposition temperature of $LiCoO_2$ [27–30]. The utilization of these salts is mainly to reduce the decomposition temperature of $LiCoO_2$ and improve the leaching efficiency of lithium and cobalt. These studies have reduced the energy consumption of traditional recovery methods and the use of strong acid/alkali reagents to a certain extent. However, most of the existing $LiCoO_2$ recovery research is still limited to the extraction and recovery of valuable metals or preparation of corresponding precursors, while few attempts have been conducted for the high-value utilization of the product. The focus of current studies on $LiCoO_2$ is to increase the charging cut-off voltage to realize its theoretical capacity (274 mAh/g). $LiCoO_2$ is actually an aged cathode materials with numerous consumptions, if we could convert spent $LiCoO_2$ into high-voltage $LiCoO_2$ with a novel recovery method that avoids shortcomings of current recycling processes, it will bring significant inspiration to the studies on recycling of all kinds of cathode materials [31–36].

Following this line, we developed a closed-loop recycling method focused on cathode materials that converts spent $LiCoO_2$ into $LiCoO_2$ with stable cyclability at 4.5 V for LIBs without utilization of high temperature roasting and corrosive agents. This strategy is different from previous closed-loop recycling method, which only aimed at extraction of metal elements and preparation of ordinary $LiCoO_2$ [29]. The decomposition temperature of $LiCoO_2$ was reduced below 400 ˚C with the assistance of ammonium sulfate. The spent $LiCoO_2$ cathode was transformed into soluble components after low-temperature roasting, which was then leached in water and separated by the addition of inexpensive sodium carbonate. Lithium component was finally converted to $Li_2CO_3$ by selective evaporation and cobalt component was extracted as $Co_3O_4$, which were then used for the synthesis of high-voltage $LiCoO_2$. The recovery efficiencies of lithium and cobalt exceeded 90%, and the possible profit of the entire recycling process approached 6.94 $/kg cell. This proposed study provides a novel closed-loop strategy for sustainable recycling of $LiCoO_2$.

## 2. Results and discussions

### 2.1. Comparative analysis of spent $LiCoO_2$ and commercial $LiCoO_2$

Herein, we established a closed-loop recycling route to not only extract the metallic components but also re-combine them back into $LiCoO_2$ with improved performances as illustrated in Fig. 1a. In order to gain a deep understanding for the recovery and re-synthesis of $LiCoO_2$, we first analyzed the changes of spent $LiCoO_2$ compared with the commercial $LiCoO_2$. Commercial $LiCoO_2$ has very good crystallinity while many miscellaneous peaks could be observed in spent $LiCoO_2$ (Fig. 1b). The long-term charging and discharging led to lithium loss in spent $LiCoO_2$, exhibiting a Li/Co molar ratio of only 0.786, deviating from stoichiometric ratio. In contrast, the Li/Co ratio of commercial $LiCoO_2$ is 0.986 (Fig. 1c). As for morphology, the crystal micro-structure may be collapsed after long-term cycling as many noticeable micro-cracks are observed in spent $LiCoO_2$ (Fig. 1d), which is in consistent with XRD results. The particle sizes of spent $LiCoO_2$ are also not uniform. In contrast, a smooth surface with uniform particle size distribution are observed for commercial $LiCoO_2$ (Fig. 1e). A schematic diagram for lattice structure of commercial $LiCoO_2$ and spent $LiCoO_2$ is thus summarized in Fig. 1f, showing a considerable amount of vacancies caused by lithium loss. Time-of-flight secondary ion mass spectrometry (TOF-SIMS) images of spent $LiCoO_2$ also shows obvious cracks with exposure of high amount of Li (Fig. 1g). In contrast, commercial $LiCoO_2$ is more uniform in particle size and Li distribution with no cracks at edges (Fig. 1h). Their particle size distributions were also comparatively analyzed: commercial $LiCoO_2$ is more concentrated with a smaller median diameter (~10 μm), while the distribution of spent $LiCoO_2$ is more dispersed with a larger median diameter (~14 μm) (Fig. S1). Raman spectrum of spent $LiCoO_2$ has approximately identical characteristic peaks as that of commercial $LiCoO_2$, but the base line is coarser, implying a worse crystallinity related to XRD results (Fig. S2). In short, the structure and composition of spent $LiCoO_2$ exhibit significant changes from commercial $LiCoO_2$, which disqualified itself from being re-used as cathode directly.

### 2.2. Reaction mechanism between $LiCoO_2$ and $(NH_4)_2SO_4$

$LiCoO_2$ and $(NH_4)_2SO_4$ were mixed with different molar ratios from 1:0.5 to 1:3, and the optimized ratio was 1:2 according to XRD results (Figs. S3-S5). $LiCoO_2$ and $(NH_4)_2SO_4$ mixed with this ratio, as well as $LiCoO_2$ and $(NH_4)_2SO_4$ separately, were analyzed by thermogravimetry (Fig. 2a). $LiCoO_2$ is very stable in the air and does not decompose even if heated to 1000 ˚C. In contrary, $(NH_4)_2SO_4$ begins to decompose at about 220 ˚C, and it is completely decomposed at 420 ˚C. The TG curves of their mixture contains three characteristic peaks during 220 to 420 ˚C. The reaction mechanism between $LiCoO_2$ and $(NH_4)_2SO_4$ was quite complicated, which may involve dozens of chemical reactions and various intermediate products. Therefore, we conducted an *in-situ* XRD measurement on mixture of $LiCoO_2$ and $(NH_4)_2SO_4$ from room temperature to 500 ˚C and analyzed specific intermediate products at 250, 300, 350 and 400 ˚C to identify the phases of transition products to infer the reaction mechanism (Figs. 2b-c) [28]. Overall, the multiple reactions began from 200 ˚C, where the main peak of the $LiCoO_2$ and $(NH_4)_2SO_4$ disappeared, which coincide with the results of TG curves. The characteristic peaks of $(NH_4)_2SO_4$ and $LiCoO_2$ are identified under the roasting temperature of 250 ˚C, indicating an incomplete reaction process. When the roasting temperature is increased to 300 ˚C, the characteristic peaks of $(NH_4)_2SO_4$ and $LiCoO_2$ disappear, which have been transformed into complex intermediate products, including $Li_2Co(SO_4)_2$, $Li_2S_2O_6$, $Li_2SO_4$, $CoSO_4$, etc. It can be seen that the lithium element is not completely converted into simple $Li_2SO_4$, so does the cobalt element. However, the valence state of lithium is +1, while cobalt has been reduced from trivalent in $LiCoO_2$ to divalent in all of the various products, which is extremely important for the dissolution of cobalt element in water.

To further analyze the reaction mechanism, we combined the results of TG and XRD to speculate possible chemical reactions and the corresponding Gibbs free energies. According to the TG curve, the reaction process is divided into three steps. The first step is completely coincident with the TG curve of $(NH_4)_2SO_4$, so the first reaction during 220 to 320 ˚C is obviously the decomposition of $(NH_4)_2SO_4$, as shown in Eq. (1).

$$(NH_4)_2SO_4\ (s)=2NH_3\ (g)+H_2SO_4\ (l) \quad (1)$$

This is the critical step why $LiCoO_2$ could be decomposed at low temperatue. The decomposition of $(NH_4)_2SO_4$ will release free high-energy $H^+$, which could disintegrate the structure of $LiCoO_2$ to allow subsequent reactions to occur [28]. Complicated reactions between $LiCoO_2$ and sulfuric acid ($H^+$) occur with temperature increasing from 320 to 370 ˚C. We speculate that the possible processes contains decompsotion of $LiCoO_2$ into $Li_2O$ and CoO, reactions between $Li_2O$ or CoO and sulfuric acid, as shown in Eqs. (2-4):

$$4LiCoO_2\ (s) = 2Li_2O\ (s)+4CoO\ (s)+O_2\ (g) \quad (2)$$

$$Li_2O\ (s)+H_2SO_4\ (l) = Li_2SO_4\ (s)+H_2O\ (g) \quad (3)$$

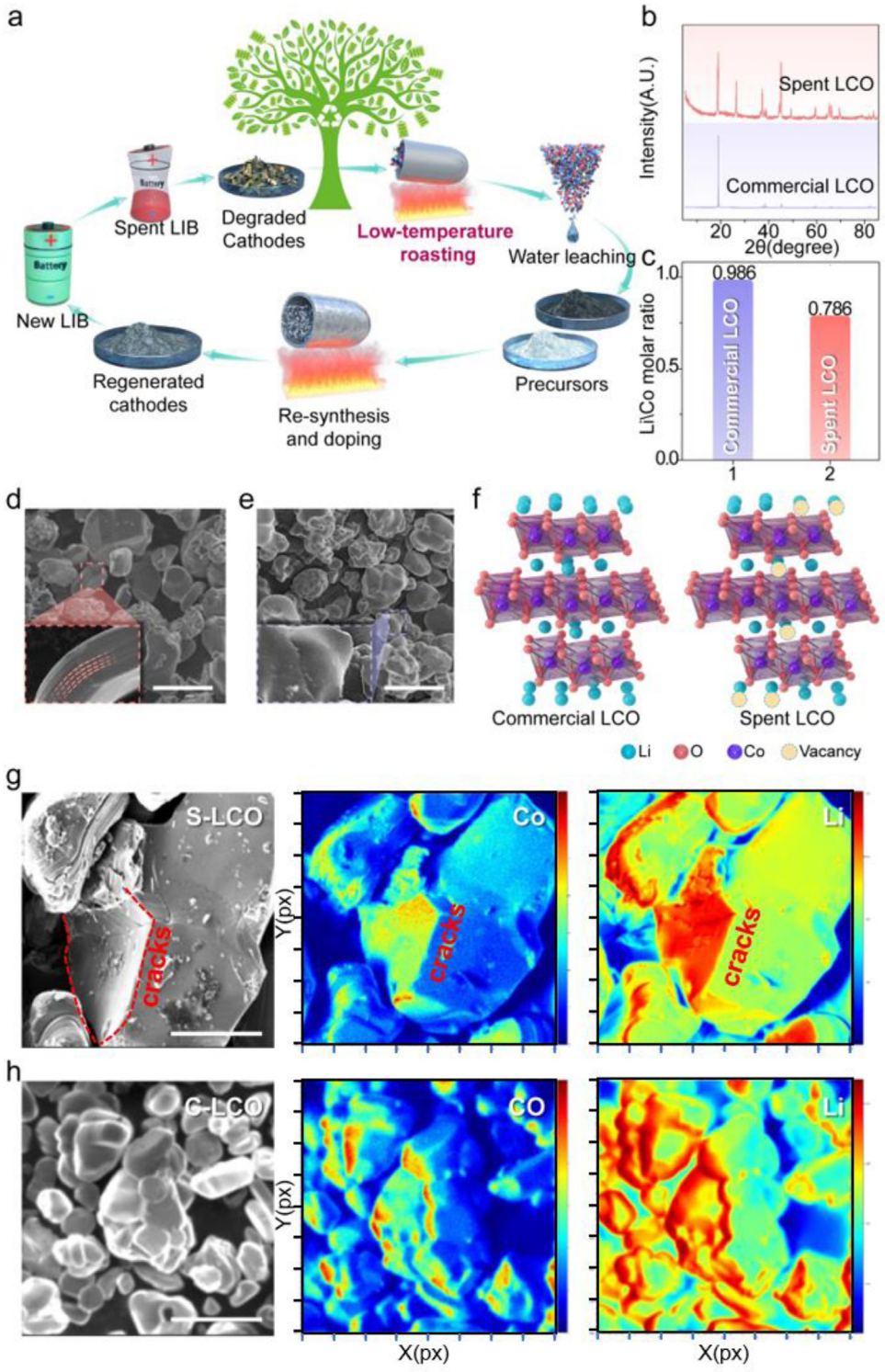


**Fig. 1.** (a) The proposed closed-loop recycling process to convert spent $LiCoO_2$ into high-voltage $LiCoO_2$. b XRD patterns of spent $LiCoO_2$ and commercial $LiCoO_2$. c Li/Co molar ratio of spent $LiCoO_2$ and commercial $LiCoO_2$. d SEM images of spent $LiCoO_2$ (Scale bar = 5 μm). e SEM images of commercial $LiCoO_2$ (Scale bar = 5 μm). f Schematic of lattice structure of spent $LiCoO_2$ and commercial $LiCoO_2$. g TOF-SIMS image of spent $LiCoO_2$ and element distribution of Co and Li (Scale bar = 1 μm). h TOF-SIMS image of commercial $LiCoO_2$ and element distribution of Co and Li (Scale bar = 1 μm).

$$CoO\ (s)+H_2SO_4\ (l) = CoSO_4\ (s)+H_2O\ (g) \quad (4)$$

Therefore, the overall chemical reaction could be concluded by combining Eqs. (2-4) to Eq. (5):

$$4LiCoO_2\ (s)+6H_2SO_4\ (l) = 2Li_2SO_4\ (s)+4CoSO_4\ (s)+6H_2O\ (g)+O_2\ (g) \quad (5)$$

The Gibbs energies of these reactions were calculated, as shown in Fig. 2d. When the temperature exceeds approximately 230 °C, the Gibbs energies of all reactions will drop below 0, indicating that these reactions could occur. It is worth mentioning that the thermodynamic data of some products cannot be obtained from the HSC chemistry database, especially these complex intermediate products (such as $Li_2Co(SO_4)_2$, $Li_2S_2O_6$). However, these intermediate products can be regarded as a combination of $Li_2SO_4$ and $CoSO_4$, which does not cause weight loss. For example, $Li_2Co(SO_4)_2$ could be formed by reaction of $Li_2SO_4$ and $CoSO_4$:

$$Li_2SO_4\ (s)+\ CoSO_4\ (s) = Li_2Co(SO_4)_2\ (s) \quad (6)$$

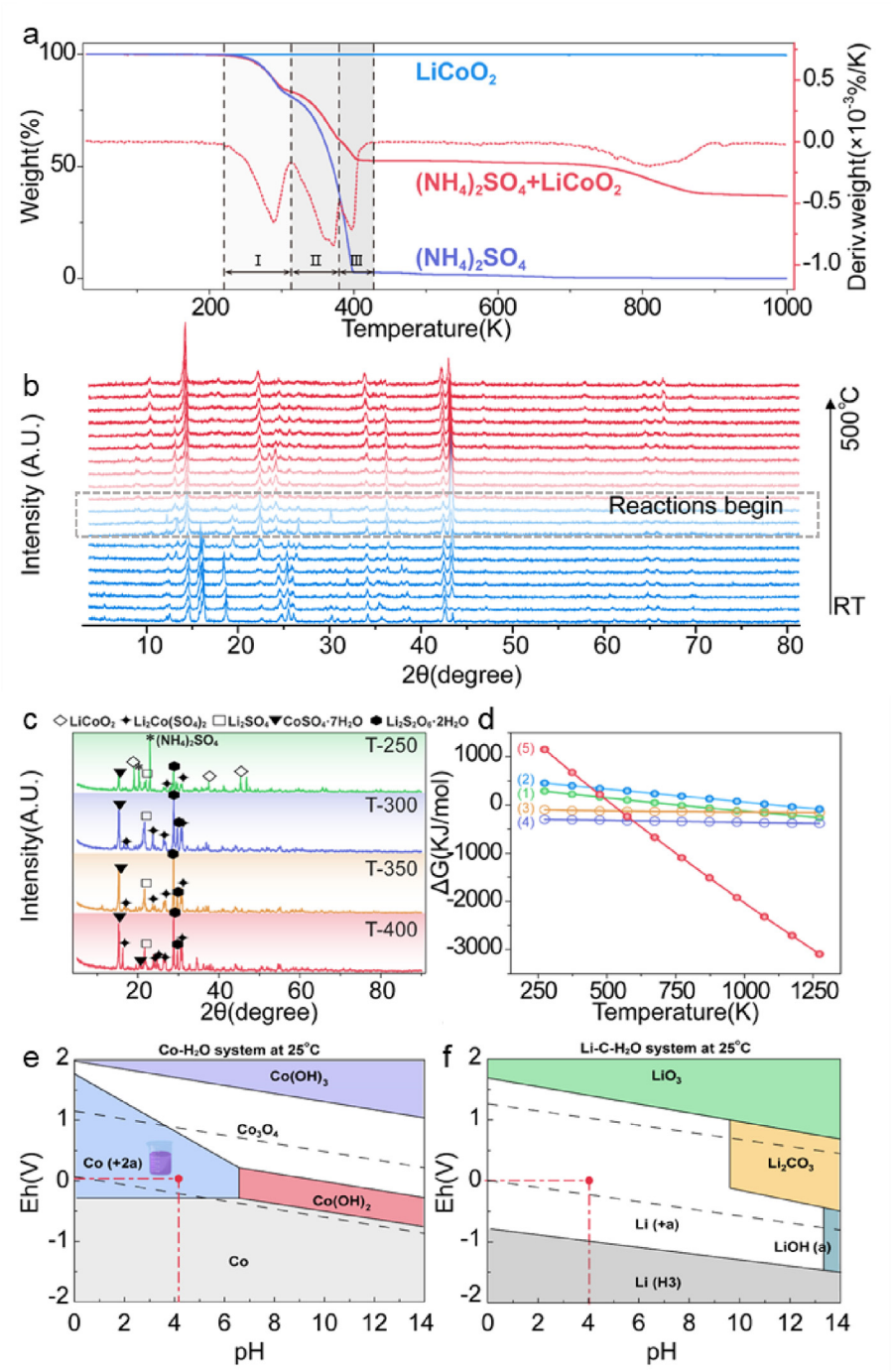


**Fig. 2.** (a) TG curves of $LiCoO_2$, $(NH_4)_2SO_4$, and their mixture; b *in-situ* XRD patterns of roasting products from room temperature to 500 °C; c specific XRD patterns of roasting products at different temperatures; d Gibbs energies of the proposed chemical reactions; e E-pH diagram of Co-$H_2O$ systems; f E-pH diagram of Li-C-$H_2O$ systems.

$Li_2S_2O_6$ is the reaction product of $Li_2SO_4$ and excess sulfuric acid as follows:

$$2LiCoO_2(s)+4H_2SO_4(l) = Li_2S_2O_6{\cdot}2H_2O(s)+2CoSO_4(s)+2H_2O(g)+O_2(g) \quad (7)$$

Eq. (5) occurs completely with a weight loss of 22.1%, while Eq. (7) occurs completely with a weight loss of 9.6%. The actual weight loss from TG analysis is 21.7%, indicating that the two reactions may occur simultaneously. There is a small weight loss between 370 and 420 °C, which may correspond to the complete decomposition of residual sulfuric acid [37].

To sum up, $LiCoO_2$ is completely decomposed to a mixture of lithium salt and divalent cobalt salt after a series of complex reactions. The mixture is weakly acidic after being dissolved in water, and the measured pH is about 4.2. Coincidentally, divalent cobalt exists in water as an ion, while lithium exists in water as a monovalent ion according to the E-pH phase diagrams of Li-C-$H_2O$ and Co-$H_2O$ systems at this condition (Figs. 2e and f). The previous work did not provide an explanation for the water solubility of the roasted mixture [28], and the corresponding theoretical analysis was supplemented in this manuscript. Therefore, the mixture can be directly leached with water, which provides dramatic convenience for subsequent element extraction.

### *2.3. Re-synthesis of high-voltage $LiCoO_2$ and its electrochemical performance*

The lithium and cobalt were extracted via addition of low-cost $Na_2CO_3$ for preparation of $Li_2CO_3$ and $Co_3O_4$ precursors, which were

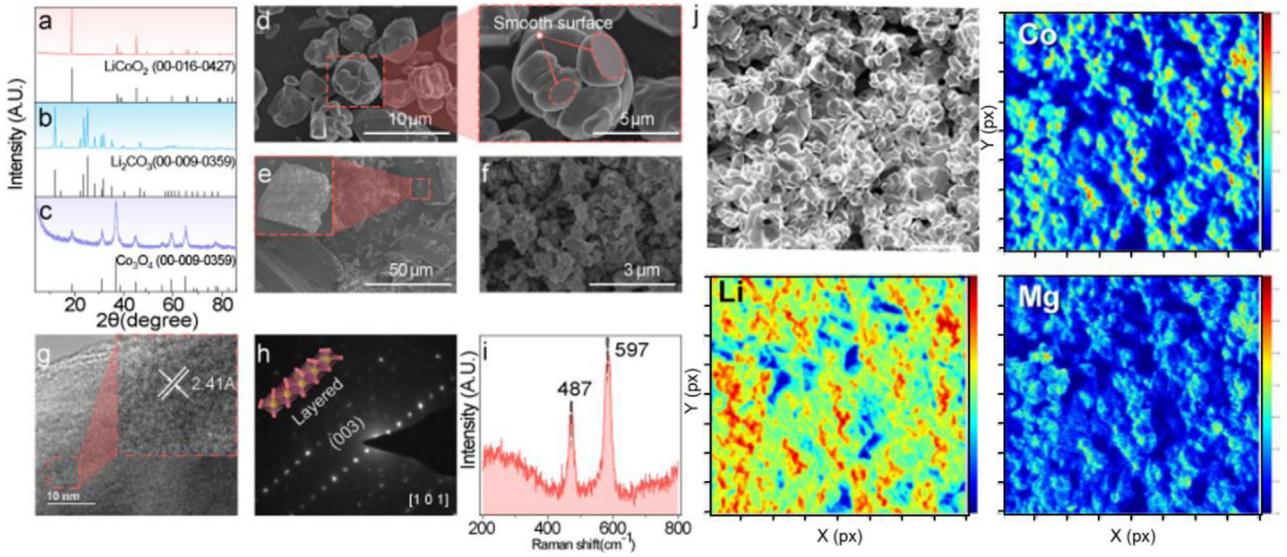


**Fig. 3.** (a) XRD pattern of re-synthesized $LiCoO_2$; b XRD pattern of $Li_2CO_3$ precursor; c XRD pattern of $Co_3O_4$ precursor; d SEM images of re-synthesized $LiCoO_2$; e SEM image of $Li_2CO_3$ precursor; f SEM image of $Co_3O_4$ precursor; g HRTEM images, the corresponding interplanar spacing and h SAED pattern of re-synthesized $LiCoO_2$; i Raman spectra of re-synthesized $LiCoO_2$. j TOF-SIMS images of re-synthesized $LiCoO_2$ and element distribution of Li, Co and Mg (Scale bar = 10 μm).

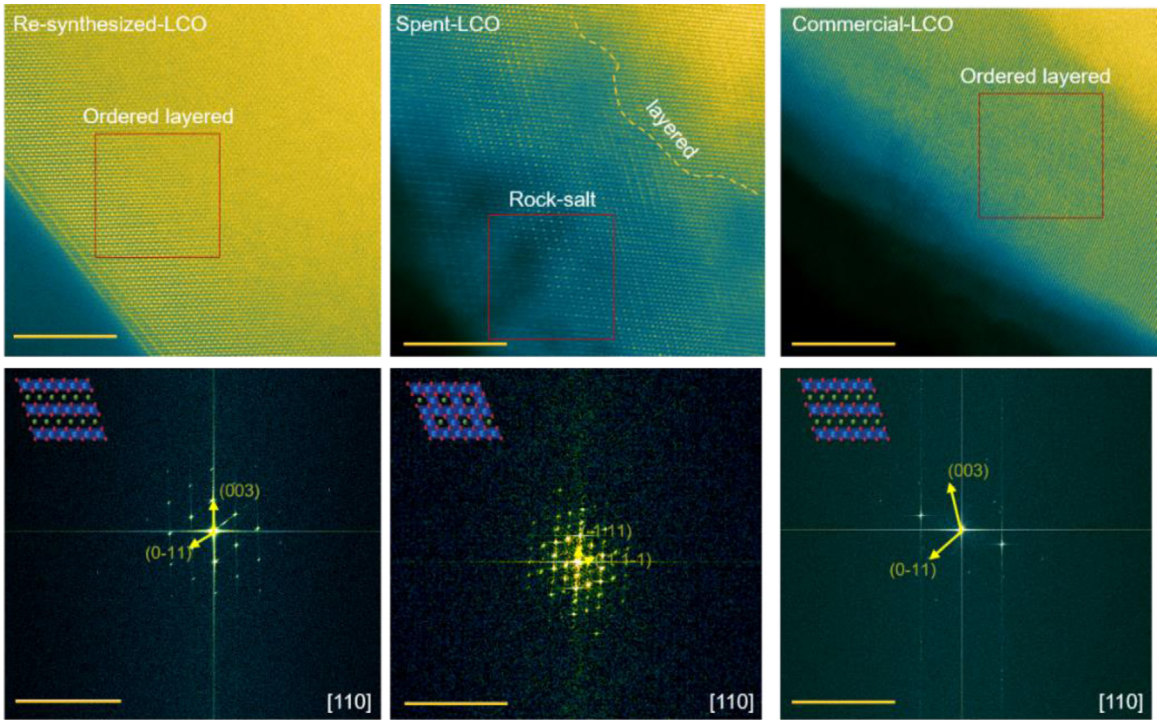


**Fig. 4.** HAADF-STEM images of re-synthesized $LiCoO_2$, spent $LiCoO_2$ and Commercial $LiCoO_2$ and the corresponding SAED images (scale bar = 5 nm).

used for re-synthesis of $LiCoO_2$. The re-synthesized $LiCoO_2$ has a layered $\alpha$-$NaFeO_2$ structure under the space group *R3m* as standard $LiCoO_2$ (Fig. 3a). In addition, the $Li_2CO_3$ crystals are large in size and show columnar shapes, while $Co_3O_4$ exhibits an amorphous morphology, which are similar to previous reports. Meanwhile, their XRD pattern match with standard cards well [38,39] (Fig. 3b and c, e and f). The re-synthesized $LiCoO_2$ has a grain size of several micrometers and a smooth surface (Fig. 3d), which is completely different from the spent $LiCoO_2$ (Fig. 1d). The molar ratio of O/Co of re-synthesized $LiCoO_2$ was 2.1, measured by EDX, which is identical to its stoichiometric value (Fig. S6). No corresponding peaks related to Na was detected in re-synthesized $LiCoO_2$. It has an ordered layered structure verified by SAED pattern and an interplanar spacing of 2.41 Å related to plane (101) (Fig. 3g and h). The Raman spectra of re-synthesized $LiCoO_2$ shows flat baseline with characteristic peaks at 487 and 597 $cm^{-1}$, implying an ordered layered crystal structure similar to commercial $LiCoO_2$ (Fig. 3i and S2) [40]. The re-synthesized $LiCoO_2$ has uniform size and morphology. Although the content of Mg element is less than 1 wt%, it is still evenly distributed (Fig. 3j). The re-synthesized $LiCoO_2$ exhibits an ordered layered lattice structure similar to commercial $LiCoO_2$, while in spent $LiCoO_2$,

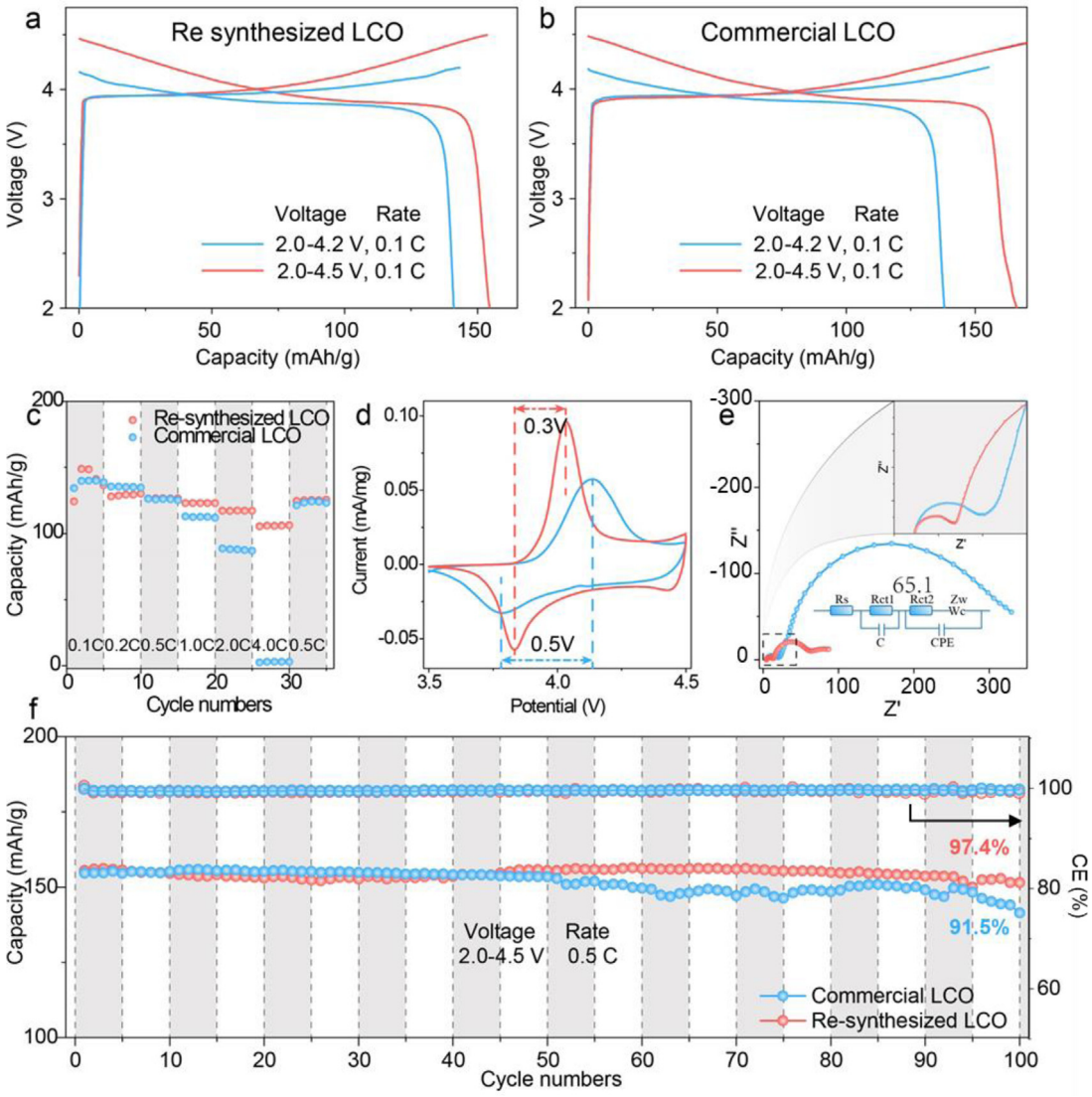


**Fig. 5.** (a) Charging and discharging curves of re-synthesized $LiCoO_2$ at 4.2 and 4.5 V; b Charging and discharging curves of commercial $LiCoO_2$ at 4.2 and 4.5 V; c Rate capabilities of commercial $LiCoO_2$ and re-synthesized $LiCoO_2$; d CV curves of re-synthesized $LiCoO_2$ and commercial $LiCoO_2$; e EIS spectra of re-synthesized $LiCoO_2$ and commercial $LiCoO_2$; f Cycling performance of commercial $LiCoO_2$ and re-synthesized $LiCoO_2$ at 4.5 V.

a mixed lattice structure of layered and rock-salt could be observed (Fig. 4). An element mapping based on STEM images of re-synthesized $LiCoO_2$ is shown in Fig. S7, demonstrating a homogeneous distribution of Mg.

The charging and discharging curves of re-synthesized $LiCoO_2$ and commercial $LiCoO_2$ at different voltages were compared in Fig. 5a and b. The re-synthesized $LiCoO_2$ delivers an initial capacity of 142.1 and 154.3 mAh/g at 4.2 and 4.5 V, respectively, which are comparable to those of commercial $LiCoO_2$ (138.7 mAh/g at 4.2 V, and 155.1 mAh/g at 4.5 V). While the rate capability of re-synthesized $LiCoO_2$ is much better (141.2 mAh/g at 0.1 C, and 105.9 mAh/g at 4 C) than commercial $LiCoO_2$ (139.9 mAh/g at 0.1 C, and only 2.9 mAh/g at 4 C). The trace doping of $MgF_2$ has significantly improved the high-rate capability (Fig. 5c). The evenly distributed $Mg^{2+}$ helps to stabilize bulk structure for rapid diffusion of $Li^+$, which contributes to the improved rate capability. As for electrochemical performances, the re-synthesized $LiCoO_2$ shows excellent electrochemical activity compared with commercial $LiCoO_2$ (Fig. 5d). The oxidation and reduction peaks of the re-synthesized $LiCoO_2$ are located at nearly 4.1 V and 3.8 V, showing a difference of 0.3 V. As for commercial $LiCoO_2$, the oxidation and reduction peaks are located at 4.2 V and 3.7 V, with a difference of 0.5 V, indicating worse reversibility compared with re-synthesized $LiCoO_2$. The impedance of re-synthesized $LiCoO_2$ is also smaller than commercial $LiCoO_2$, owing to trace doping of $Mg^{2+}$ (Fig. 5e). The cycling performances of re-synthesized $LiCoO_2$ and commercial $LiCoO_2$ are shown in Fig. 5f. The re-synthesized $LiCoO_2$ shows better cycling stability than commercial $LiCoO_2$ under cut off voltages of both 4.2 and 4.5 V (Figs. S8 and 5f). The capacity retention rate of re-synthesized $LiCoO_2$ reaches 97.4% at 4.5 V. As a comparison, the capacity retention rate of commercial $LiCoO_2$ is only 91.5% at 4.5 V. This result is better than that of most of the current studies of $Mg^{2+}$ doping $LiCoO_2$ at charging cut-off voltage of 4.5 V (Fig. S9). In conclusion, the re-synthesized $LiCoO_2$ demonstrates excellent performance, especially outstanding cycling performance under high-voltage conditions. This result is mainly attributed to the $MgF_2$ doping. When $LiCoO_2$ is charged to high voltage up to 4.5 V, $Co^{4+}$ with high activity will be produced along with the de-intercalation of $Li^+$. $Co^{4+}$ will react with electrolyte easily once they contact each other, leading to the dissolution of cobalt and impair on structural stability. A small amount of $MgF_2$ have a coating effect on the surface of $LiCoO_2$ particles, thereby preventing direct contact of $Co^{4+}$ and electrolyte. Therefore, the structural stability and cycling performance of $LiCoO_2$ under high voltage is greatly improved.

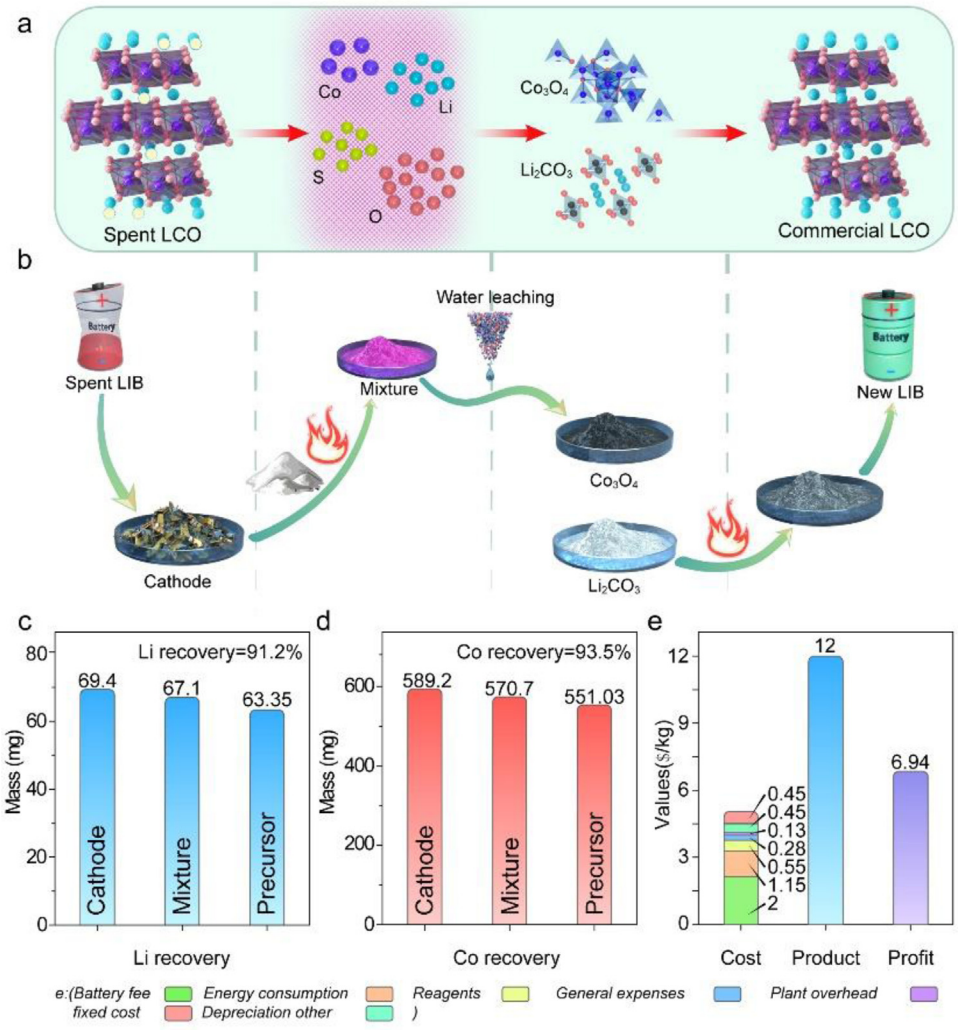


**Fig. 6.** (a) Schematic of the proposed recycling process; b Detailed recycling process and the corresponding products of each step; c Mass of Li element in different steps; d Mass of Co element in different steps; e Estimated cost, product value and potential profit of this method.

### 2.4. Economic analysis of the recycling process

Economic benefit is a key factor that determines whether a recycling method can be widely promoted. Therefore, we conducted a brief economic analysis on this closed-loop recycling method. The brief schematic of this proposed recycling process is summarized in Fig. 6a and b. The proposed recycling process contains three roasting steps and two filtration steps (Fig. S10). We have measured the mass of products and the concentration of each element during each step. 1 g of spent $LiCoO_2$ contains 69.4 mg of Li, and 67.1 mg of Li was measured in the roasted mixture. Finally, 63.4 mg of Li was obtained in filtrate after filtration (Fig. 6c), indicating a recovery efficiency of 91.3%. As for Co element, 589.2 mg was contained in 1 g of spent $LiCoO_2$, and 570.7 mg of Co element was measured in the roasted mixture. Finally, 551.0 mg of Co was obtained in residue after filtration (Fig. 6d), showing a recovery efficiency of 93.5%. The loss of lithium and cobalt is mainly caused by the residues in the filtration and mass transfer process. With the expansion of the reaction scale, the recovery rate can be further improved. The specific mass and concentrations during each step are provided in Table S1.

In order to estimate the cost and possible benefits of this method, we assume the recycling of 1 kg spent LIB cells according to the above recovery rate. The cost of a spent LIB is 2 $/kg cell according to database in EverBatt 2020 model, and the weight of the cathode in a battery was calculated as 30%, which is 300 g accordingly. Six moles of $(NH_4)_2SO_4$, 792 g in total, is consumed during roasting, and 4.5 mol of $Na_2CO_3$ (477 g), is added after roasting. Eventually, approximately 280 g of re-synthesized $LiCoO_2$ can be reproduced, and 1wt% of $MgF_2$ (2.8 g) was used as dopants. The price for industrial grade $(NH_4)_2SO_4$ is about 538.5 $/t, while $Na_2CO_3$ and $MgF_2$ cost 230.8 $/t and 4.7 $/kg. As for energy consumption, the electric furnace power is 2.5 kW, which consumes 5 kwh of electricity after two hours roasting (the price is 0.23 $/kWh). This recycling method has basically the same requirements for equipment as the traditional pyrometallurgical process, so no extra cost of equipment is needed. Some other costs including general expenses (0.28 $/kg cell), plant overhead (0.13 $/kg cell), other fixed cost (0.51 $/kg cell), and depreciation (0.45 $/kg cell) are approximately the same as pyrometallurgical process according to EverBatt 2020 model (Table S2). Moreover, no additional treatment costs are required since there is no waste water produced. The total cost was calculated as 5.06 $/kg cell based on the above assumption and simulation, and the price of high-voltage $LiCoO_2$ is currently about 43,000 $/t. Therefore, recycling 280 g of high-voltage $LiCoO_2$ can generate a value of about 12 $/ kg cell, and the potential profit reaches about 6.94 $/kg cell after subtracting the direct cost, which is considerable (Fig. 6e). Due to the high value of high-voltage $LiCoO_2$, low-temperature roasting, and water leaching process, the cost of this method is effectively reduced and the potential benefits is higher than some currently reported methods (Fig. S11). It should be noted that our calculations here are only based on existing data and simulations, therefore leading to a relative rough estimation

for reference, which may not reflect the real benefit during practical implementation. However, this closed-loop recycling method has the following advantages such as simple procedures, low-cost reagents, and high-value products, thereby holds great potential economic benefits.

## 3. Conclusions

In this work, we propose a closed-loop and green recycling strategy for spent $LiCoO_2$ cathodes based on low temperature roasting combined with water leaching. In this recycling approach, use of both acid and alkali was avoided with no wastewater produced. Moreover, 91.3% of lithium and 93.5% of cobalt from spent $LiCoO_2$ were recovered and converted directly to high-voltage $LiCoO_2$ which was adopted back into the battery as cathodes. The re-synthesized $LiCoO_2$ shows better cycling performance under a high-voltage of 4.5 V than commercial $LiCoO_2$. In addition to the aforementioned advantages, use of low-cost reagents, high recovery efficiency, and concept of circular economy make this recycling strategy extremely promising with great profitability. In summary, direct conversion of spent cathodes into high performance $LiCoO_2$ with high recovery efficiency, lower energy consumption, no wastewater produced, non-corrosive and inexpensive reagents, opens a new direction for Li-ion battery recycling.

## 4. Material and methods

### 4.1. Chemicals and reagents

The spent LIBs were first soaked in a sodium chloride solution until the output voltage dropped to 2 V. It was then rinsed and dried, manually disassembled into different parts including cathodes, anodes, and separators. The spent cathodes comprising current collector (Al foil) and active materials were ground into small pieces and soaked in 1 M sodium hydroxide solution with continuous stirring at room temperature for 12 h to remove Al foil. The mixed solution was then filtrated to obtain the residue that contains $LiCoO_2$, polyvinylidene fluoride (PVDF) and acetylene black. The as-obtained residue was dried and heated at 500 ˚C for 2 h to remove PVDF. The spent $LiCoO_2$ was thereby obtained for subsequent use. The chemical reagents, including sodium hydroxide (NaOH, AR, 99.0%), sodium chloride (NaCl, AR, 99.0%), ammonium sulfate ($(NH_4)_2SO_4$, AR, 99.0%), sodium carbonate ($Na_2CO_3$, AR, 99.0%), magnesium fluoride ($MgF_2$, AR, 99%), PVDF (AR, 99%), and N-methyl-pyrrolidone (NMP, AR, 99%) were purchased from Macklin Co. Ltd. and used without further treatment. Commercial $LiCoO_2$ from Kluthe Co. Ltd. was used as comparison.

### 4.2. The recycling and re-synthesis processes

A specific amount of $(NH_4)_2SO_4$ and $LiCoO_2$ were mixed and ground in a mortar for 10 mins. The molar ratio between $(NH_4)_2SO_4$ and $LiCoO_2$ was ranged from 0.5:1 to 3:1. The mixture was then transferred into a crucible for roasting under different temperatures ranging from 250 to 400 ˚C. The roasting procedure lasted for 2 to 4 h, and the whole roasting process was optimized to guarantee complete decomposition of spent $LiCoO_2$. The roasting process would generate $NH_3$, which was absorbed by post position water solution. The optimized conditions are as follows: the molar ratio of $(NH_4)_2SO_4$ and $LiCoO_2$ is 2:1, the roasting temperature is 400 ˚C, and the reaction time is 1 h (Table S3). The mixture after roasting was purple in color and soluble in water. A specific amount of $Na_2CO_3$ solution was added into the purple solution, and precipitation was formed rapidly. The mixed solution was filtrated and the as-obtained residue containing $Co^{2+}$ was heated in air at 350 ˚C to generate $Co_3O_4$, while the transparent filtrate was evaporated to obtain $Li_2CO_3$ (Fig. S12). $Li_2CO_3$ has a completely opposite solubility to that of general salts. That is, the higher the temperature, the lower the solubility, while the solubility of $Na_2SO_4$ increases significantly. Therefore, heating the solution to 100 ˚C to reduce its volume to about one-tenth of its original volume can allow more than 95% of the $Li_2CO_3$ to precipitate out while the $Na_2SO_4$ remains in the solution. $Na_2SO_4$ solution could be obtained for further reutilization after separation of $Li_2CO_3$.

For the re-synthesis process, $Li_2CO_3$ and $Co_3O_4$ from the above recycling process were ground in a mortar, and the molar ratio of Li: Co is 1.03:1 to compensate lithium loss during high temperature sintering (Fig. S13). The re-synthesis process of high-voltage $LiCoO_2$ consists of three steps. The mixture was first sintered at 850 ˚C for 10 h, and then sintered at 920 ˚C for another 10 h. However, the capacity of the as-formed bare $LiCoO_2$ was only 120 mAh/g at 0.1 C with a limited cycling performance, so it must be improved for high-voltage applications (Figs.S14 and 15). Therefore, a trace amount of $MgF_2$ was doped in synthesized $LiCoO_2$ for an extra sintering step at 800 ˚C for 6 h to effectively stabilize the cycling performance at high-voltage [35,36]. The final obtained $LiCoO_2$ was rinsed with water for several times to remove possible impurities. The same amount of $MgF_2$ was also added to commercial $LiCoO_2$ to improve its cycling stability (Fig. S16).

### 4.3. Electrochemical performance test

The re-synthesized $LiCoO_2$ or commercial $LiCoO_2$ were mixed with carbon blacks (Denka Black Li-400) in a mortar by grinding for 30 mins. PVDF dissolved in NMP was then added into the mixture for another 30 mins of stirring. The mass ratio of $LiCoO_2$, carbon blacks, and PVDF was 8:1:1. The slurry was obtained and coated on an Al foil with a mass loading of approximately 5 mg/cm$^2$. The coated Al foil was dried under vacuum at 80 ˚C for 12 h. The dried plate was then cut into small round pieces with a diameter of 12 mm for assembling of CR2032 coin cells. Metallic lithium chips were selected as anode and separators were purchased from Celgard. $LiFP_6$ dissolved in ethylene carbonate (EC)/dimethyl carbonate (DMC) with a volume ratio of 50/50 was utilized as electrolyte. The sealed coin cells were tested via a Lanhe battery testing system at room temperature. The rate capabilities were conducted at 0.1, 0.2, 0.5, 1.0, 2.0, and 4.0 C, and the charging cut off voltage was set to 4.2 V (versus Li/Li$^+$). The cycling performances at charging cut off voltages of 4.2 and 4.5 V (versus Li/Li$^+$) were all tested at a current of 0.5 C. The cyclic voltammetry (CV) curves of different $LiCoO_2$ samples were conducted on Chi760 electrochemical workstation at a scan rate of 0.1 mV/s with a voltage ranging from 3.5 to 4.5 V.

### 4.4. Materials characterizations

The crystalline phases of different samples were characterized by X-ray diffraction (XRD, D8 Advance) with Cu K$\alpha$ radiation at a scanning rate of 5˚/minute. Scanning electron microscopy (SEM, Hitachi SU8010) was used to observe the morphology of $LiCoO_2$ and different precursors. The molar ratios of Li and Co in different $LiCoO_2$ samples were also measured by inductively coupled plasma optical emission spectrometer (ICP-OES 8300, Arcos II MV) after a complete dissolution via utilization of 5 M $HNO_3$ and 30% v/v $H_2O_2$. Particle size distribution of different $LiCoO_2$ samples were analyzed by laser particle size analyzer, and Raman spectra was acquired by Horiba LabRAM HR800. Thermogravimetric (TG) analysis of $LiCoO_2$, $(NH_4)_2SO_4$ and their mixture were conducted via thermogravimetric analyzer (TG209F3 Nevio). Gibbs energies of assumed reaction and E-pH diagrams were all collected and reproduced from database in HSC chemistry 6.0.

## Declaration of Competing Interest

The authors declare that they have no known competing financial interests or personal relationships that could have appeared to influence the work reported in this paper.

## CRediT authorship contribution statement

**Junxiong Wang:** Conceptualization, Writing – original draft, Writing – review & editing. **Zheng Liang:** Supervision, Conceptualiza-

tion, Visualization, Resources, Writing – review & editing. **Yun Zhao:** Methodology. **Jinzhi Sheng:** Methodology. **Jun Ma:** Methodology. **Kai Jia:** Methodology. **Baohua Li:** Methodology. **Guangmin Zhou:** Supervision, Conceptualization, Validation, Writing – review & editing. **Hui-Ming Cheng:** Supervision, Resources, Writing – review & editing.

## Acknowledgement

G.Z appreciates support from the National Key Research and Development Program of China (2019YFA0705700), National Natural Science Foundation of China (No. 52072205), start-up funds of Tsinghua Shenzhen International Graduate School and Shenzhen Geim Graphene Center. Z. L. acknowledges the financial support from the start-up funds of Shanghai Jiao Tong University. The authors would like to thank the Testing Technology Center of Materials and Devices of Tsinghua Shenzhen International Graduate School, Kaifeng Carbon Accademy of Advanced Materials, and Feringa Nobel Prize Scientist Joint Research Center for their help on materials characterizations.

## Supplementary materials

Supplementary material associated with this article can be found, in the online version, at doi:10.1016/j.ensm.2021.12.013.

## References

[1] Y.-.C. Lyu, X. Wu, K. Wang, Z. Feng, T. Cheng, Y. Liu, M. Wang, R.-.M. Chen, L.-.M. Xu, J.-.J. Zhou, Y.-.H. Lu, B.-.K. Guo, An Overview on the Advances of $LiCoO_2$ Cathodes for Lithium-Ion Batteries, Adv. Energy Mater. 11 (2021) 2000982, doi:10.1002/aenm.202000982.

[2] L. Wu, W.H. Lee, J. Zhang, First principles study on the electrochemical, thermal and mechanical properties of $LiCoO_2$ for thin film rechargeable battery, Mater. Today 1 (2014) 82–93, doi:10.1016/j.matpr.2014.09.017.

[3] S. Luo, K. Wang, J. Wang, K. Jiang, Q. Li, S. Fan, Binder-free $LiCoO_2$/carbon nanotube cathodes for high-performance lithium ion batteries, Adv. Mater. 24 (2012) 2294–2298, doi:10.1002/adma.201104720.

[4] K. Yamada, Cobalt: its Role in Health and Disease. In: Sigel A., Sigel H., Sigel R. (eds) Interrelations Between Essential Metal Ions and Human Diseases. Metal Ions in Life Sciences, vol 13. Springer, Dordrecht, 2013, https://doi.org/10.1007/978-94-007-7500-8_9.

[5] L. Leyssens, B. Vinck, C. Van Der Straeten, F. Wuyts, L. Maes, Cobalt toxicity in humans-a review of the potential sources and systemic health effects, Toxicology 387 (2017) 43–56, doi:10.1016/j.tox.2017.05.015.

[6] M.-.K. Jha, A. Kumari, A.-.K. Jha, V. Kumar, J. Hait, B.-.D. Pandey, Recovery of lithium and cobalt from waste lithium ion batteries of mobile phone, Waste Manage. 33 (2013) 1890–1897, doi:10.1016/j.wasman.2013.05.008.

[7] C. Liu, J. Lin, H. Cao, Y. Zhang, Z. Sun, Recycling of spent lithium-ion batteries in view of lithium recovery: a critical review, J. Clean. Prod. 228 (2019) 801–813, doi:10.1016/j.jclepro.2019.04.304.

[8] E. Fan, L. Li, Z. Wang, J. Lin, Y. Huang, Y. Yao, R. Chen, F. Wu, Sustainable recycling technology for Li-ion batteries and beyond: challenges and future prospects, Chem. Rev. 120 (2020) 7020–7063 doi: 10.1021 /acs. chemrev. 9b 00535.

[9] M. Chen, X. Ma, B. Chen, R. Arsenault, P. Karlson, N. Simon, Y. Wang, Recycling end-of-life electric vehicle lithium-ion batteries, Joule 3 (2019) 2622–2646, doi:10.1016/j.joule.2019.09.014.

[10] Y. Yang, E.-.G. Okonkwo, G. Huang, S. Xu, W. Sun, Y. He, On the sustainability of lithium ion battery industry–a review and perspective, Energy Storage Mater. 36 (2020) 186–212, doi:10.1016/j.ensm.2020.12.019.

[11] G. Harper, R. Sommerville, E. Kendrick, L. Driscoll, P. Slater, R. Stolkin, A. Walton, P. Christensen, O. Heidrich, S. Lambert, A. Abbott, K. Ryder, L. Gaines, P. Anderson, Recycling lithium-ion batteries from electric vehicles, Nature 575 (2019) 75–86, doi:10.1038/s41586-019-1682-5.

[12] J. Piątek, S. Afyon, T.-.M. Budnyak, S. Budnyk, M.-.H. Sipponen, A. Slabon, Sustainable Li-Ion Batteries: chemistry and Recycling, Adv. Energy Mater. (2020) 2003456, doi:10.1002/aenm.202003456.

[13] E. Antolini, $LiCoO_2$: formation, structure, lithium and oxygen nonstoichiometry, electrochemical behaviour and transport properties, Solid State Ionics 170 (2004) 159–171, doi:10.1016/j.ssi.2004.04.003.

[14] J. Mao, J. Li, Z. Xu, Coupling reactions and collapsing model in the roasting process of recycling metals from $LiCoO_2$ batteries, J. Clean. Prod. 205 (2018) 923–929 doi: j.jclepro.2018.09.098.

[15] J. Li, Y. Lai, X. Zhu, Q. Liao, A. Xia, Y. Huang, X. Zhu, Pyrolysis kinetics and reaction mechanism of the electrode materials during the spent $LiCoO_2$ batteries recovery process, J. Hazard. Mater. 398 (2020) 122955, doi:10.1016/j.jhazmat.2020.122955.

[16] G. Zhang, X. Yuan, Y. He, H. Wang, W. Xie, T. Zhang, Organics removal combined with in situ thermal-reduction for enhancing the liberation and metallurgy efficiency of $LiCoO_2$ derived from spent lithium-ion batteries, Waste Manage. 115 (2020) 113–120, doi:10.1016/j.wasman.2020.05.030.

[17] Y. Yao, M. Zhu, Z. Zhao, B. Tong, Y. Fan, Z. Hua, Hydrometallurgical processes for recycling spent lithium-ion batteries: a critical review, ACS Sustain. Chem. Eng. 6 (2018) 13611–13627, doi:10.1021/acssuschemeng.8b03545.

[18] D. Yang, T. Gu, H. Zhou, J. Zeng, Z. Jiang, Study on the leaching of $LiCoO_2$ in low $H_2SO_4$ concentration solutions, Adv. Mater. Res. 201 (2011) 1752–1756, doi:10.4028/www.scientific.net/AMR.201-203.1752.

[19] P. Zhang, T. Yokoyama, O. Itabashi, T.M. Suzuki, K. Inoue, Hydrometallurgical process for recovery of metal values from spent lithium-ion secondary batteries, Hydrometallurgy 47 (1998) 259–271, doi:10.1016/S0304-386X(97)00050-9.

[20] J. Myoung, Y. Jung, J. Lee, Y. Tak, Cobalt oxide preparation from waste $LiCoO_2$ by electrochemical–hydrothermal method, J. Power Sources 112 (2002) 639–642, doi:10.1016/S0378-7753(02)00459-7.

[21] B. Wang, X.-.Y. Lin, Y. Tang, Q. Wang, M. Leung, X.-.Y. Lu, Recycling $LiCoO_2$ with methanesulfonic acid for regeneration of lithium-ion battery electrode materials, J. Power Sources 436 (2019) 226828 doi: 10.1016/j. jpowsour. 2019.226828.

[22] D. Patil, S. Chikkamath, S. Keny, V. Tripathi, J. Manjanna, Rapid dissolution and recovery of Li and Co from spent $LiCoO_2$ using mild organic acids under microwave irradiation, J. Environ. Manage. 256 (2020) 109935, doi:10.1016/j.jenvman.2019.109935.

[23] G. Nayaka, Y. Zhang, P. Dong, D. Wang, K.-.V. Pai, J. Manjanna, G. Santhosh, J. Duan, Z. Zhou, J. Xiao, Effective and environmentally friendly recycling process designed for $LiCoO_2$ cathode powders of spent Li-ion batteries using mixture of mild organic acids, Waste Manage. 78 (2018) 51–57, doi:10.1016/j.wasman.2018.05.030.

[24] S. Refly, O. Floweri, T.-.R. Mayangsari, A. Sumboja, S.-.P. Santosa, T. Ogi, F. Iskandar, Regeneration of $LiNi_{1/3}Co_{1/3}Mn_{1/3}O_2$ Cathode Active Materials from End-of-Life Lithium-Ion Batteries through Ascorbic Acid Leaching and Oxalic Acid Coprecipitation Processes, ACS Sustain. Chem. & Eng. 8 (2020) 16104–16114, doi:10.1021/acssuschemeng.0c01006.

[25] P. Meshram, A. Mishra, R. Sahu, Environmental impact of spent lithium ion batteries and green recycling perspectives by organic acids–a review, Chemosphere 242 (2020) 125291, doi:10.1016/j.chemosphere.2019.125291.

[26] A. Verma, G.-.H. Johnson, D.-.R. Corbin, M.-.B. Shiflett, Separation of Lithium and Cobalt from $LiCoO_2$: a Unique Critical Metals Recovery Process Utilizing Oxalate Chemistry, ACS Sustain. Chem. Eng. 8 (2020) 6100–6108, doi:10.1021/acssuschemeng.0c01128.

[27] X. Qu, H. Xie, X. Chen, Y. Tang, B. Zhang, P. Xing, H. Yin, Recovery of $LiCoO_2$ from spent lithium-ion batteries through a low-temperature ammonium chloride roasting approach: thermodynamics and reaction mechanisms, ACS Sustain. Chem. Eng. 8 (2020) 6524–6532, doi:10.1021/acssuschemeng.0c01205.

[28] S. He, B.-.P. Wilson, M. Lundstrom, Z. Liu, Clean and efficient recovery of spent $LiCoO_2$ cathode material: water-leaching characteristics and low-temperature ammonium sulfate calcination mechanisms, J. Clean. Prod. 268 (2020) 122299, doi:10.1016/j.jclepro.2020.122299.

[29] Y. Tang, H. Xie, B. Zhang, X. Chen, Z. Zhao, J. Qu, P. Xing, H. Yin, Recovery and regeneration of $LiCoO_2$-based spent lithium-ion batteries by a carbothermic reduction vacuum pyrolysis approach: controlling the recovery of CoO or Co, Waste Manage. 97 (2019) 140–148, doi:10.1016/j.wasman.2019.08.004.

[30] H. Dang, N. Lia, Z. Chang, B. Wang, Y. Zhan, X. Wu, W. Liu, S. Ali, H. Li, J. Guo, W. Li, H. Zhou, C. Sun, Lithium leaching via calcium chloride roasting from simulated pyrometallurgical slag of spent lithium ion battery, Sep. Purif. Technol. 233 (2020) 116025, doi:10.1016/j.seppur.2019.116025.

[31] Q. Liu, X. Su, D. Lei, Y. Qin, J. Wen, F. Guo, Y.-.A. Wu, Y. Rong, R. Kou, X. Xiao, F. Aguesse, J. Bareño, Y. Ren, W. Lu, Li Y, Approaching the capacity limit of lithium cobalt oxide in lithium ion batteries via lanthanum and aluminium doping, Nat. Energy 3 (2018) 936–943, doi:10.1038/s41560-018-0180-6.

[32] J. Zhang, Q. Li, C. Ouyang, X. Yu, M. Ge, X. Huang, E. Hu, C. Ma, S. Li, R. Xiao, W. Yang, Y. Chu, Y. Liu, H. Yu, X. Yang, X. Huang, L. Chen, Li H, Trace doping of multiple elements enables stable battery cycling of LiCoO2 at 4.6V, Nat. Energy 4 (2019) 594–603, doi:10.1038/s41560-019-0409-z.

[33] J. Qian, L. Liu, J. Yang, S. Li, X. Wang, H.-.L. Zhuang, Y. Lu, Electrochemical surface passivation of $LiCoO_2$ particles at ultrahigh voltage and its applications in lithium-based batteries, Nat. Commun. 9 (2018) 1–11, doi:10.1038/s41467-018-07296-6.

[34] Z. Zhu, H. Wang, Y. Li, R. Gao, X. Xiao, Q. Yu, C. Wang, I. Waluyo, J. Ding, A. Hunt, J. Li, A Surface Se-Substituted $LiCo[O_{2-\delta}Se_{\delta}]$ Cathode with Ultrastable High-Voltage Cycling in Pouch Full-Cells, Adv. Mater. 32 (2020) 2005182, doi:10.1002/adma.202005182.

[35] Y. Huang, Y. Zhu, H. Fu, M. Ou, C. Hu, S. Yu, Z. Hu, C. Chen, G. Jiang, H. Gu, H. Lin, W. Luo, Y. Huang, Mg-pillared $LiCoO_2$: towards Stable Cycling at 4.6V, Angew. Chem. Int. Edit. 132 (2020) 2–9, doi:10.1002/ange.202014226.

[36] K.-.D. Du, Y.-.F. Meng, X.-.X. Zhao, X.-.T. Wang, X.-.X. Luo, W. Zhang, X.-.L. Wu, A unique co-recovery strategy of cathode and anode from spent $LiFePO_4$ battery, Sci. China Mater. (2021) 1–9, doi:10.1007/s40843-021-1772-6.

[37] C. Huang, T. Ali, Analysis of sulfur–iodine thermochemical cycle for solar hydrogen production. Part I: decomposition of sulfuric acid, Sol. Energy 78 (2005) 632–646, doi:10.1016/j.solener.2004.01.007.

[38] T. Nakamura, A. Kajiyama, Synthesis of $LiCoO_2$ particles with uniform size distribution using hydrothermally precipitated $Co_3O_4$ fine particles, Solid State Ionics 123 (1999) 95–101, doi:10.1016/S0167-2738(99)00114-9.

[39] T. Ohzuku, A. Ueda, Solid-state redox reactions of $LiCoO_2$ ($R_{3m}$) for 4volt secondary lithium cells, J. Electrochem. Soc. 141 (1994) 2972 doi: 10.1149/1.2059267/meta#.

[40] H. Porthault, R. Baddour-Hadjean, C. Le, F.-.C. Bourbon, S. Franger, Raman study of the spinel-to-layered phase transformation in sol–gel $LiCoO_2$ cathode powders as a function of the post-annealing temperature, Vib. Spectrosc. 62 (2012) 152–158, doi:10.1016/j.vibspec.2012.05.004.